PHYSICAL REVIEW B VOLUME 37, NUMBER 12 15 APRIL 1988-II

Multiple-scattering effects in surface extended x-ray absorption fine structure

D. Arvanitis, K. Baberschke, and L. Wenzel
Institut für Atom- und Festkörperphysik, Freie Universität Berlin, D-1000 Berlin 33, Federal Republic of Germany
(Received 15 December 1987)

A multiple-scattering approach is used in the analysis of the surface extended x-ray absorption fine structure (SEXAFS) oscillations of O and N on Ni(100) and O on Ni(110) and Cu(110). As a result details about the reconstruction of N and O on Ni and Cu are obtained. The analysis demonstrates for the first time that a single-scattering approach for low-Z SEXAFS is not adequate.

In recent years x-ray photoelectron spectroscopy has proven to be among the most effective means of surface structure characterization. The possibility of multiple-scattering (MS) contributions has been considered very early in angle-resolved photoemission experiments of adsorbate core levels in order to improve the agreement to the experiment.[1] Many different traveling paths for the outgoing scattered photoelectron wave interfere and contribute to the yield under a fixed angle and kinetic energy. For a photoabsorption coefficient measurement the interference between outgoing and scattered photoelectron waves takes place at the absorber atom site. One is then sensitive only to closed-loop photoelectron paths, from the excited to the neighbor atoms and back. Close to the absorption threshold energy, in the near edge region, MS contributions are important, due to the longer mean-free path of the photoelectron. They can yield reliable surface structural information by comparing calculations to the experiment.[2] For the extended x-ray absorption fine structure (EXAFS) in the bulk, MS contributions are also known.[3,4] Only for the surface EXAFS[5] of light elements, the single-scattering (SS) approach has been used up to date. Here we prove for the first time on a systematic way for low-Z adsorbate systems the importance of MS contributions. It involves more complicated photoelectron paths than to the nearest neighbors and back. We prove that if MS contributions are taken into account, more structural parameters of the adsorbate-substrate system can be obtained, yielding valuable new information on surface reconstruction models.[6]

We use the theory obtained for the K-edge EXAFS of a three-atom system in a plane-wave approximation:[7]

$$\chi(k) = -\sum_{i,j} \frac{3(\hat{\mathbf{e}}\cdot\hat{\mathbf{r}}_i)^2}{kr_i^2}|f_i(\pi)|\sin(2kr_i+2\delta+\phi_i) - 6\frac{(\hat{\mathbf{e}}\cdot\hat{\mathbf{r}}_i)(\hat{\mathbf{e}}\cdot\hat{\mathbf{r}}_j)}{kr_ir_jr_{ij}}|f_i(\alpha_i)|\,|f_j(\alpha_j)|\sin[k(r_i+r_j+r_{ij})+2\delta+\phi_i+\phi_j]$$
$$-3\frac{(\hat{\mathbf{e}}\cdot\hat{\mathbf{r}}_j)^2}{kr_j^2r_{ij}^2}|f_i(\pi)|\,|f_j(\alpha_j)|^2\sin[2k(r_j+r_{ij})+2\delta+\phi_i+2\phi_j]\ , \qquad (1)$$

where the absorber is located at the origin of the coordinate system. The first term in Eq. (1) is the usual SS contribution [Fig. 1(a): $1\rightarrow 3\rightarrow 1$]. The second and third terms are MS contributions [Fig. 1(a): $1\rightarrow 3\rightarrow 2\rightarrow 1$, $1\rightarrow 4\rightarrow 3\rightarrow 1$, etc.]. δ and ϕ_i are the phase shifts due to the absorber and scatterer at r_i. If one focuses on higher-order shells with longer photoelectron paths the MS contributions may overcome the SS ones, if the geometry is favorable (α close to 0° or 180°). This is in particular the case for adsorbates sitting close to the surface. The effect of a finite photoelectron mean free path ($\lambda \simeq 5$ Å) has also been taken into account but is not shown in Eq. (1). The frequency of the MS contributions and their relative amplitude with respect to SS can be estimated using theoretical calculations[3,8,9] for δ, ϕ_i, and $f_i(\alpha_i)$ for the different elements. In the case of surface EXAFS, with submonolayer adsorbate coverages and low photon fluxes at the C, N, and O K edges, poor statistics have not allowed, until recently,[5] the identification of longer photoelectron paths out of the noise, than to the first nearest neighbor and back. If one analyzes the nearest-neighbor (NN) peak in the fast Fourier transform (FFT) only, the SS approach is fully justified. In the present Communication, we discuss recent high-quality data, for low-Z adsorbates on metal surfaces. For more than one SEXAFS oscillation, it is important to take into account different MS and SS photoelectron paths and the possibility of destructive interference. In the following we demonstrate our new approach for the SEXAFS analysis for (2×1)O on Ni(110) and Cu(110) and for a $c(2\times2)$ overlayer of N and O on Ni(100).

Figures 1 and 2 recall the local adsorption geometry for (2×1)O/Ni(110). An earlier SEXAFS study[10(a)] concluded a sawtooth (ST) model for the reconstructed Ni(110) surface, but left features in the FFT related to longer photoelectron paths unanswered [peak B in Fig. 2(a)]. Using Eq.(1), we calculated the various EXAFS contributions (Table I, columns 1 and 2). With this input we simulated the experimental oscillations for geometries close to the one proposed in Ref. 10. The possible destructive interference effects between different contributions and the limited k-range effects in the FFT are taken into account. According to the angle α_i the MS scattering amplitude $f_i(\alpha_i,k)$ can be different from the SS one.[3,9] In

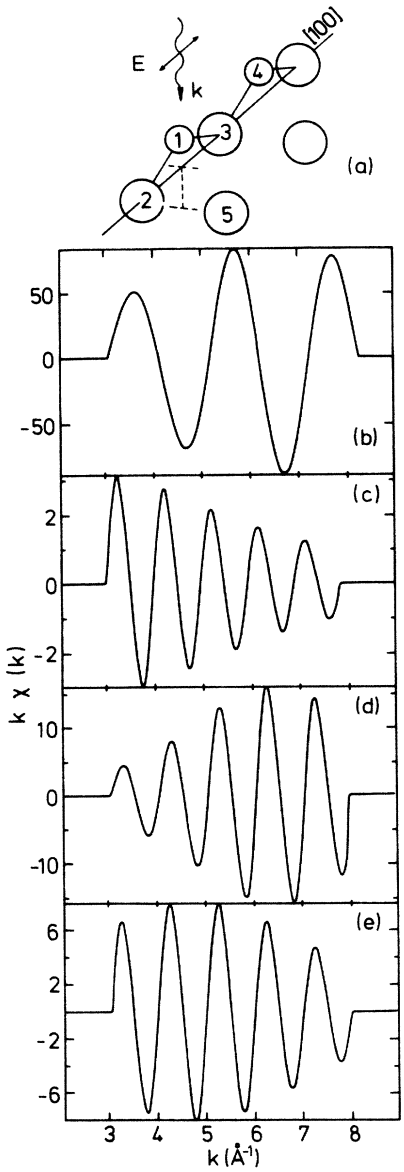

FIG. 1. (a) Schematic local geometry of (2×1)O/Ni(110) (small circles: oxygen) and **E** parallel to the [100] direction. EXAFS contributions $\chi(k)$ relative to scale: (b) O-Ni NN contribution SS ($1 \rightarrow 3 \rightarrow 1$). (c) The O-O SS contribution ($1 \rightarrow 4 \rightarrow 1$) peaks at very low k. (d) The MS of O-Ni-Ni ($1 \rightarrow 3 \rightarrow 2 \rightarrow 1$) has its maximum at $k \approx 6$ to 7 Å^{-1}. (e) For a mixed MS of O-Ni-O ($1 \rightarrow 4 \rightarrow 3 \rightarrow 1$) the maximum is in between.

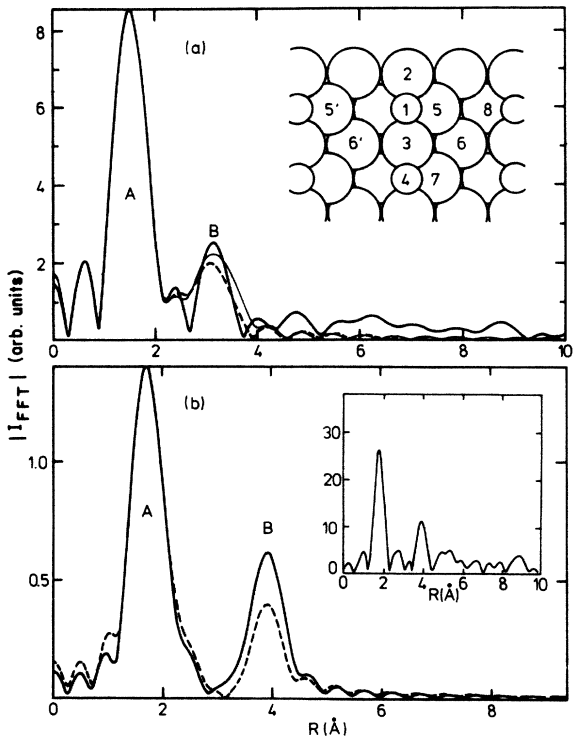

FIG. 2. FFT modulus $|I_{FFT}|$ of experimental and simulated SEXAFS oscillations. (a) O/Ni(110): experimental FFT (thick solid line) [Ref. 10(a)]. Simulated FFT of 6 contributions (thin solid line). Simulated FFT of only $\chi(k)$ shown in Figs. 1(d) and 1(e) for peak *B* (dashed line). The difference between the thin solid and dashed line shows nicely that the less important contributions have larger paths from 8 to 8.6 Å. Note that the ST model is asymmetric, the symmetric lattice site to atom 5 (inset) is vacant. (b) O/Cu(110): the full line is a simulation for a ST reconstruction and the dashed for a MR. The *B*:*A* ratio equals 0.43 (ST) and 0.26 (MR) as can be deduced from Table I. The experimental FFT [Ref. 11(b)] is shown in the inset. The peak height ratio equals ≈ 0.42.

Fig. 1(b) the O-Ni single scattering shows the largest amplitude *f*. The second largest contributions are the MS effects in Figs. 1(d) and 1(e). The SS of O-O [Fig. 1(c)] is seven to four times smaller than the dominant MS. The peak *B* in the FFT of Fig. 2 is dominated by MS of the Ni NN, rather than by SS of O-O. The thin solid line in Fig. 2(a) shows the simulation for six contributions including geometrical paths up to 8.64 Å. The dashed line at peak *B* shows the r_{1431} and r_{1321} contributions only. A small change in the first NN distance will now affect also the position and amplitude of peak *B*. It is therefore possible to check the first NN distance and obtain new information concerning Ni-Ni and O-O atom distances included in the closed-loop triangle photoelectron paths, responsible for peak *B*. In this case the lattice constant of bulk Ni agrees well to the total photoelectron path length. As a result of our calculation the structural model proposed in Ref. 10(a) is confirmed within experimental error.[10(b)] We find that a unique phase[8] fits all peaks satisfactorily, if one included MS effects.

The case of (2×1)O/Cu(110) is very close to the previous system, the same bridge site [Fig. 1(a)] was determined by virtue of the azimuthal angular dependence of SEXAFS.[11(a)] Recently[11(b)] experiments with better statistics show more than one peak in the FFT, in particular for the *E* vector parallel to [110] [inset of Fig. 2(b)]. A SS analysis[11(b)] concluded a missing-row (MR) reconstruction. In view of the extreme sensitivity of the high-frequency long photoelectron paths to small structural changes and the possible destructive interference effects that can ensue, we used the MS theory and simulated the FFT for a MR and ST model [Fig. 2(b)]. The simulation

TABLE I. In column 2 are shown the photoelectron traveling distances (see Fig. 1 to Fig. 3 for labels) with the amplitudes of the relevant contributions to the SEXAFS oscillations. The amplitudes in column 2 are calculated using Eq. (1) in atomic units. Nevertheless, only ratios can be compared to the experiment. The amplitudes are shown at the point of maximum intensity in k space (e.g., Fig. 1). Columns 3 and 4 show the peak position and amplitude of the FFT modulus using as an input all the contributions of the left columns (Ref. 17). For (2×1)O/Ni(110) and Cu(110) and **E** parallel to [110], columns 2 and 4 show the contributions for a ST reconstruction. For a MR model one needs to multiply the amplitude in column 2 for $1\rightarrow 5\rightarrow 1$, $1\rightarrow 5\rightarrow 6\rightarrow 1$, and $1\rightarrow 5'\rightarrow 1$ by a factor of 2. The result is given in parentheses in column 4. Column 5 and 6 show the experimental data [Refs. 10(a), 11(b), and 13]. For convenience the most intense SS peak for each system is given with the same figure as in column 4. The experimental error bars are 10% for O/Cu [Ref. 11(b)] and ≈ 20% for all the other systems [Refs. 10(a) and 13].

	Theory		FFT Simulation		FFT experiment	
	Path (Å)	Amplitude	Peak (Å)	Amplitude	Peak (Å)	Amplitude
			(2×1)O/Ni(110)			
					$E\parallel$[100]	
r_{121}	3.60	0.887	1.42	0.887	1.42	0.887
r_{1321}	7.12	0.163	3.19	0.304	3.19	0.23
r_{1431}	7.12	0.132				
r_{141}	7.04	0.032				
r_{1371}	8.30	0.071				
					E∥[110]	
r_{151}	3.82	0.122	1.66	0.139 ST	1.66	0.17
r_{1561}	8.46	0.017	3.98	(0.278) MR	3.69	0.045
$r_{15'1}$	8.46	0.027		0.046 ST		
r_{161}	8.11	0.025		(0.101) MR		
$r_{16'1}$	8.55	0.025				
			(2×1)O/Cu(110)			
					E∥[110]	
r_{151}	3.98	0.146	1.73	0.166 ST	1.73	0.25
r_{1561}	8.74	0.021	3.93	(0.322) MR	3.93	0.11
$r_{15'1}$	8.22	0.031		0.072 ST		
$r_{16'1}$	8.38	0.049		(0.086) MR		
			c(2×2)O/Ni(100)			
					E∥[110]	
r_{131}	3.96	0.618	1.75	0.618	1.75	0.62
r_{1341}	6.43	0.073	2.69	0.108	2.76	0.10
			$p4g$(2×2)N/Ni(100)			
					E∥[110]	
r_{131}	3.78	0.869	1.67	0.869	1.67	0.87
r_{1341}	6.50	0.100	2.65	0.104	2.85	0.12

for a ST model yields an amplitude ratio of 0.43 in agreement with the experiment [see inset of Fig. 2(b)]. *This is the most striking example for the importance of MS and interference:* in the SS model [see Ref. 11(b)] there are two times more backscattering atoms responsible for peak B than in a ST model. The dashed line in Fig. 2(b) should be two times more intense than the full line for peak B. In our present MS analysis other atoms (5 and 6) are also responsible for peak B and the interference produces a higher intensity for a ST model. It is not the purpose of the present Communication to discriminate uniquely between the ST and MR reconstruction. We are just comparing the experimental results of Ref. 11(b) with the present simulation. However, on that basis we come to the conclusion that the chemically induced reconstruction by oxygen creates in both cases a ST reconstruction.

We now focus on the Ni(100) substrate. For c(2×2)O/Ni(100), $p4g$N/Ni(100) (Fig. 3), and $p4g$C/Ni(100) (Refs. 12–15) the adsorbate atoms occupy a fourfold hollow site (insets of Fig. 3). The experimental FFT shows a second peak around 2.8 Å. Using Eq. (1) we find that a closed-loop triangle path (Fig. 3, $1\rightarrow 3\rightarrow 4\rightarrow 1$, Table I) is again responsible for the second peak (for simulation see Fig. 4 in Ref. 6).

If the previously determined experimental geometry for the on-reconstructed system c(2×2)O/Ni(100) is used as an input,[13] the MS of the Ni-O-Ni relevant loop can be determined experimentally, as there is in this case only one triangle loop contribution to the MS peak in the Fourier transform, in contrast to the previous cases on the (110) faces. The determined MS phase $2\delta_O+2\phi_{Ni}=2.7-0.85k$, in good agreement to the theoretical one,[7] can now be used in order to obtain unknown distances involving the same kind of photoelectron path loop. Such a case is the $p4g$N/Ni(100) one, where upon adsorption of N the surface reconstructs.[12–14] As a result the surface lattice cell is enlarged due to a displacement of ξ of the Ni atoms around the adsorbate (Fig. 3). Using the experi-

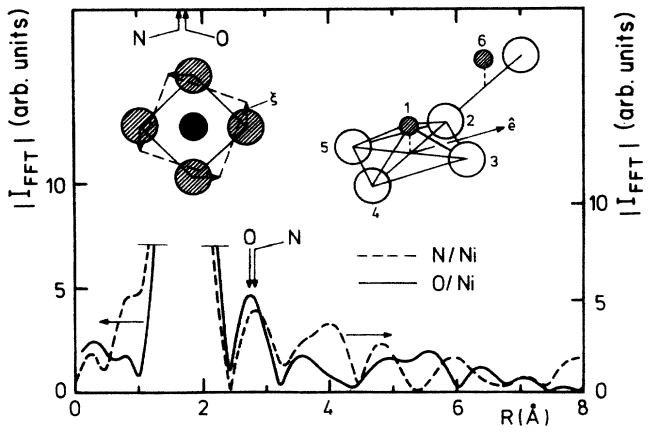

FIG. 3. The modulus of the FFT $|I_{FFT}|$ is shown for normal x-ray incidence for O and N on Ni(100). The second peak in the FFT is related to a single triangle path such as $1 \rightarrow 4 \rightarrow 3 \rightarrow 1$. The arrows indicate the position of the FFT maxima for the first and second peaks. In the case of N with a lower NN, the second peak falls at a higher distance. This can only be explained by an enlarged Ni-Ni surface lattice constant due to a N induced surface reconstruction.

mental phase we obtain for the N/Ni(100) system a photoelectron Ni-N-Ni path of 6.5 Å. The experimentally determined first N-Ni NN distance[13] of 1.89(2) Å yields a Ni-Ni distance of 2.72(5) Å and $\xi = 0.77(10)$ Å. This is the first direct experimental observation of this quantity in agreement to the indirect previous one.[13] The same reasoning after using the data of Ref. 15 would yield for the $p4g$C/Ni(100) system a $\xi \approx 0.15(20)$ Å in agreement to the smaller size of the C atoms inducing the reconstruction. The above considerations reveal the full power of a complete MS SEXAFS analysis: Ni/Ni-first-layer interatomic distances are not attainable within the SS approximation. For the low-Z adsorbate systems discussed up to now, MS effects are dominant as the adsorbate is close to the surface, for vertical heights of 0.88 Å for O/Ni(100) to 0.1 Å for C and N/Ni(100), above the surface. In cases where the adsorbate is sitting higher above the surface, from Eq. (1) it is expected that the importance of MS will decrease. In the case of C_2H_2 and C_2H_4 on Cu(100) with vertical heights around 1.3 Å,[16] we estimate MS contributions to be below 10% of the main peak intensity.

The MS analysis presented followed by simulations not only yields new structural information for the systems discussed, but considerably extends the potential of SEXAFS. The FFT of the simulated oscillations can be used as a very sensitive fingerprint in order to probe larger clusters around the adsorbate and measure first-layer substrate interatomic distances. Another field of potential applications of the MS analysis is the accurate determination of intramolecular bond lengths for chemisorbed molecules consisting of H, C, N, or O atoms. The variation of those bond lengths with respect to the gas-phase values yields important information on the chemisorption process. In this case it would be of interest to measure the SEXAFS oscillations due to the scattering of the light-Z-atom components of the molecule at the K edge of one of its constituent atoms. On a metal substrate these are dominated by the backscattering of the heavier metal atoms.[16] Using the appropriate geometry one could take advantage of MS effects involving the light Z atoms at collinear geometries to other molecular or substrate atoms. This would enhance the scattering of the light atoms and would give rise to more EXAFS oscillations for relatively small interatomic distances due to the longer MS paths.

We would like to thank J. Stöhr for bringing Ref. 7 to our attention. The work was supported by the Bundesminister für Forschung and Technologie under Grant No. 05 313 AX B-TP 2.

[1]P. J. Orders and C. S. Fadley, Phys. Rev. B **27**, 781 (1983), and references therein; J. J. Barton, S. W. Robey, and D. A. Shirley, *ibid.* **34**, 778 (1986), and references therein.

[2]D. D. Vvedensky, J. B. Pendry, U. Döbler, and K. Baberschke, Phys. Rev. B **35**, 7756 (1987).

[3]P. A. Lee and J. B. Pendry, Phys. Rev. B **11**, 2795 (1975).

[4]B. K. Teo, J. Am. Chem. Soc. **103**, 3990 (1981).

[5]P. H. Citrin, J. Phys. (Paris) Colloq. **47**, C8-437 (1986), and references therein.

[6]Part of the results have been briefly presented. K. Baberschke, in *The Structure of Surfaces II*, edited by J. S. van der Veen and M. A. Van Hove (Springer-Verlag, Berlin, 1988).

[7]J. J. Boland, S. E. Crane, and J. B. Baldeschwieler, J. Chem. Phys. **77**, 142 (1982).

[8]B. K. Teo and P. A. Lee, J. Am. Chem. Soc. **101**, 2815 (1979).

[9]M. Fink and A. Yates, At. Data **1**, 385 (1970); M. Fink and J. Ingram, *ibid.* **4**, 129 (1972); D. Gregory and M. Fink, At. Data Nucl. Data Tables **14**, 39 (1974).

[10](a) K. Baberschke, U. Döbler, L. Wenzel, D. Arvanitis, A. Baratoff, and K. H. Rieder, Phys. Rev. B **33**, 5910 (1986); (b) Here we do not concentrate on the details of the structural parameters. The best fit is obtained with: O-Ni NN distance $R_1^{00} = 1.80$ Å and a tilt angle of $\approx 30°$.

[11](a) U. Döbler, K. Baberschke, J. Haase, and A. Puschmann, Phys. Rev. Lett. **52**, 1437 (1984); (b) M. Bader, A. Puschmann, C. Ocal, and J. Haase, *ibid.* **57**, 3273 (1986).

[12]W. Daum, S. Lehwald, and H. Ibach, Surf. Sci. **178**, 528 (1986).

[13]L. Wenzel, D. Arvanitis, W. Daum, H. H. Rotermund, J. Stöhr, K. Baberschke, and H. Ibach, Phys. Rev. B **36**, 7689 (1987).

[14]J. E. Müller, W. Wuttig, and H. Ibach, Phys. Rev. Lett. **56**, 1583 (1986).

[15]M. Bader, C. Ocal, B. Hillert, J. Haase, and A. M. Bradshaw, Phys. Rev. B **35**, 5900 (1987).

[16]D. Arvanitis, L. Wenzel, and K. Baberschke, Phys. Rev. Lett. **59**, 2435 (1987).

[17]For O/Ni(110) and O/Cu(110) we have normalized to column 2 the amplitudes for the r_{121} peak. For the calculation of the first peak in the [110] direction (r_{151}) one has to take into account the incomplete polarization, consequently the figures in columns 2 and 4 are not the same.